

Quadratic Programming and Impedance Control for Transfemoral Prosthesis

Huihua Zhao, Shishir Kolathaya and Aaron D. Ames

Abstract—This paper presents a novel optimal control strategy combining control Lyapunov function (CLF) based quadratic programs with impedance control, with the goal of improving both tracking performance and the stability of controllers implemented on transfemoral prosthesis. CLF based quadratic programs have the inherent capacity to optimally track a desired trajectory. This property is used in congruence with impedance control—implemented as a feed-forward term—to realize significantly small tracking errors, while simultaneously yielding bipedal walking that is both stable and robust to disturbances. Moreover, instead of experimentally validating this on human subjects, a virtual prosthesis is attached to a robotic testbed, AMBER. The authors claim that the walking of AMBER is human like and therefore form a suitable substitute to human subjects on which a prosthetic control can be tested. Based on this idea, the proposed controller was first verified in simulation, then tested on the physical robot AMBER. The results indicate improved tracking performance, stability, and robustness to unknown disturbances.

I. INTRODUCTION

As one of the most important applications of bipedal robotic research, the development of lower-limb prosthetic devices and controllers for these devices has garnered the attention of the control and robotics communities in recent years [10], [19], [20]. Different control strategies have been utilized for the control of transtibial and transfemoral prosthetic devices. Control based on gait-pattern generators has been realized in [17], [12]. Motion intent recognition with position control is successfully implemented in [10]. With the assumption that human gait is cyclical, impedance control is also one of the common approaches [9], [11], [19].

Inspired by the large body of work related to bipedal robotic locomotion and control implementation on prosthesis, there are three basic biomechanical requirements that must be satisfied for a transtibial or transfemoral prosthesis [18], [21]: (1) the prosthetic device must support the body weight of the amputee during the stance phase, i.e., the prosthesis control should provide “stability” during the weight bearing phase; (2) the physical interface between the able body and the prosthesis must prevent undesirable pressure during locomotion. That is to say, the prosthetic controller must be “torque” optimal for the amputees wearing the device; (3) the prosthesis must mimic as nearly as possible the kinematics and dynamics of the normal gait. The amputee should be able to walk with normal appearance as the healthy people do.

The objective of this paper is to address requirements (1) and (3) indicated above, which is achieved through the following two contributions. First, we introduce the idea of using bipedal robots to test prosthetic controllers—a nominal walking gait is found for the robot that is human-like, and prosthetic controllers can be tested on a “prosthetic” leg of the robot. Through this method, we are able to present and test the second contribution of this work—a novel transfemoral prosthesis control method: control Lyapunov function (CLF) based quadratic programs (QPs) coupled with impedance control. In particular, we present a Model Independent QP (MIQP) utilizing CLFs to generate the feedback component of the controller and leverage impedance control to generate a robust feed-forward term.

Before introducing our novel prosthetic control strategy—CLF based MIQP—we first present one of the two major novel aspects of this paper: a method for testing prosthetic controllers via bipedal robots that display human-like locomotion. This allows for the collection of useful information regarding the performance of prosthetic control strategies to be gathered from the robot without the need for evasive tests on an amputee. Guided by this idea, the control strategy can be first designed and verified in simulation. With the model information of the physical robot, the essential control parameters can also be learned through simulation [3]. Then, a physical robot that has been shown to display qualitatively human-like walking, “wearing” a prosthetic device, can be used as a platform to test and polish the design of both the prosthesis controller and the prosthetic device.

With the idea of using a robot as the test platform for prosthetic control, we first show that we are able to achieve a robot walking with a prosthetic device using impedance control in both simulation and experiment. Based loosely on the definition of impedance control, first proposed by Hogan [13], the torque at each joint during a single step cycle can be represented by a series of passive impedance functions [19]. By reproducing this torque at the prosthetic device joint using the passive impedance functions, one can obtain a similar prosthetic gait compared to that found in normal gait tests. Normally, hand tuning from an expert is required to obtain the impedance parameters [8], [16], which, therefore, leads to another disadvantage—it is not optimal. Considering all the drawbacks of impedance control, the obtained tracking performance is lacking, resulting in walking that is not as robust as desired.

Utilizing the impedance controller as a feed-forward term, we present a novel control method that will be utilized for feedback to increase robustness and stability. In particular,

*This research is supported by NASA grant NNX11AN06H, NSF grants CNS-0953823 and CNS-1136104.

H. Zhao, S. Kolathaya and A. Ames are with the department of Mechanical Engineering, Texas A & M University, 3128 TAMU, College Station, USA huihuazhao, shishirny, aames@tamu.edu

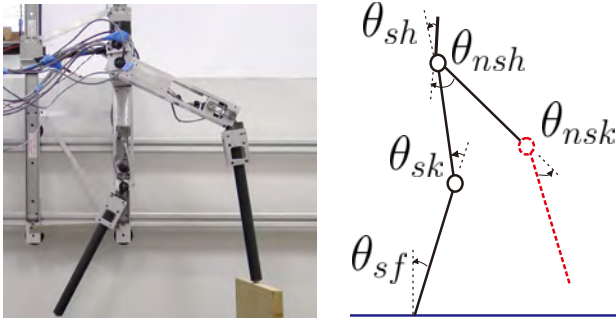


Fig. 1: The biped robot AMBER (left) and the angle conventions (right). The right leg with red dash line denotes the prosthetic device; the red dash circle represents the prosthesis joint that will be controlled using prosthetic controller.

we begin by considering rapidly exponentially stabilizing control Lyapunov functions (RES-CLFs) as introduced in [6]. This class of CLFs can naturally be stated as inequality constraints in torque such that, when satisfied, rapid exponential convergence of the error is formally guaranteed. Furthermore, these inequality constraints can naturally be solved in an optimal fashion through the use of quadratic programs. The end result is a CLF based QP as first introduced in [5]. Finally, due to the special structure of the RES-CLFs that will be considered in this paper, the CLF based QP can be stated in a model independent fashion. The end result is a novel feedback control methodology: Model Independent Quadratic Programs (MIQP) based upon RES-CLFs. These are combined with impedance control to obtain the final prosthetic controller. With the proposed controller, we will show that the tracking performance can be improved in both simulation and experiment. In addition, utilizing this novel control method, the robot displays improved stability and robustness to unknown disturbances.

The structure of this work is as follows. Both the mathematical modeling and the physical model of the robot AMBER are introduced in Sec. II. The controller constructions of the impedance control and the CLF based MIQP control are discussed in Sec. III. Simulation results, including robustness tests by using different controllers will be showed in Sec. IV. Finally, the experimental results are presented on Sec. V. Discussion and conclusion will be made in Sec. VI.

II. ROBOT MODEL

In this section, we start with a short description about the mathematical hybrid system models of bipedal robots. The physical robot, AMBER, which will be used as the test platform, is introduced at the end.

A. Robotic Model

Since the walking of bipedal robot displays both continuous and discrete dynamics, we formally represent it as a hybrid system (see [4] for a formal definition).

Continuous Dynamics. The configuration space of the robot \mathbb{Q}_R is described in body coordinates as: $\theta = (\theta_{sf}, \theta_{sk}, \theta_{sh}, \theta_{nsh}, \theta_{nsk})^T \in \mathbb{R}^5$, which are shown in Fig. 1.

With the mass and length properties corresponding to the physical robot AMBER [22], the equations of motion for the robot are given using the Euler-Lagrange formula:

$$D(\theta)\ddot{\theta} + H(\theta, \dot{\theta}) = Bu, \quad (1)$$

where $D(\theta) \in \mathbb{R}^{5 \times 5}$ is the inertial matrix including the inertia of the boom; $B \in \mathbb{R}^{5 \times 4}$ is the torque map with the consideration of underactuation, and $u \in \mathbb{R}^{4 \times 1}$, is the vector of torque inputs. Note that, since AMBER has DC motors with small inductances, we can realize the electromechanical system with voltage inputs which have the following form:

$$V_{in} = R_a i_a + K_\omega \omega, \quad (2)$$

where $V_{in} \in \mathbb{R}^{4 \times 1}$ is the vector of voltage inputs to the motors, $i_a \in \mathbb{R}^{4 \times 1}$ is the vector of currents through the motors, $R_a \in \mathbb{R}^{4 \times 4}$ is the resistance matrix, and $\omega \in \mathbb{R}^{4 \times 1}$ is the vector of motor speed which has the relation as $\omega = r_m \dot{\theta}$ with $r_m \in \mathbb{R}^{4 \times 4}$ denoting the total reduction of the system. Since the motors are controlled individually, with the torque constant $K_\phi \in \mathbb{R}^{4 \times 4}$, the applied torques are:

$$u = K_\phi R_a^{-1} (V_{in} - K_\omega \omega). \quad (3)$$

Thus, the Euler-Lagrange equation can be reformulated as:

$$D(\theta)\ddot{\theta} + H_v(\theta, \dot{\theta}) = B_v V_{in}, \quad (4)$$

where $H_v(\theta, \dot{\theta}) = H(\theta, \dot{\theta}) + K_\phi R_a^{-1} K_\omega \omega$ and $B_v = B K_\phi R_a^{-1}$. Manipulation of (4) yields the affine control system (f, g) , details of which can be found in [4].

Discrete Dynamics. A discrete impact occurs instantaneously when the swing foot hits the ground. As a result, the velocities of the robot will change, combining with a leg switch simultaneously. Impacts are assumed to be plastic as in [14], and the resulting reset map Δ_R is:

$$\Delta_R(\theta, \dot{\theta}) = \begin{bmatrix} \Delta_\theta \theta \\ \Delta_{\dot{\theta}}(\theta) \dot{\theta} \end{bmatrix}, \quad (5)$$

where Δ_θ is the relabeling which switches the stance and non-stance leg at impact, and $\Delta_{\dot{\theta}}(\theta)$ determines the change in velocities due to the impact [4].

B. AMBER Test Platform

AMBER (short for A&M Bipedal Experimental Robot) is a planar bipedal robot with 5 links (one torso, two thighs and two calves, see Fig. 1). With pointed feet configuration, AMBER is powered by 4 DC motors and is thus underactuated at the ankles. Applying the human-inspired voltage controller, AMBER has achieved stable and human-like walking in experiment [22]. In this work, we use AMBER as the platform to test the proposed prosthetic controller. The right calf is assumed to be the ‘‘prosthetic device’’ which has the same length and mass configuration of the left calf that is marked as ‘‘healthy leg’’. The proposed controller will be used on the prosthetic device, i.e., on the right knee joint. The controller for the remaining actuators will still use the original voltage P controller discussed in [22].

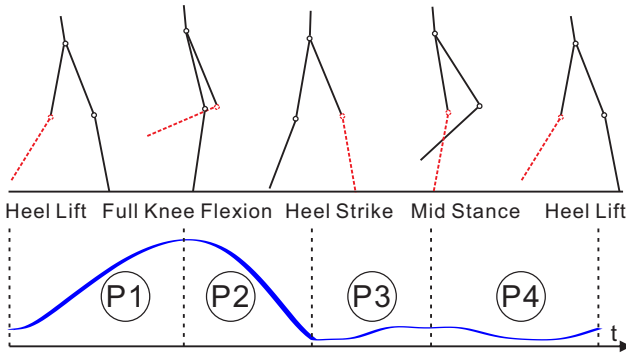


Fig. 2: AMBER gait phase separation. The red line represents the prosthetic device and the solid lines denote the able body. The green line is the knee angle of one full gait cycle.

III. CONTROLLER CONSTRUCTION

In this section, we will introduce the idea of impedance control briefly and then extend it to voltage impedance to accommodate the control of AMBER. Due to the shortcomings of impedance control, we propose the innovative CLF [6] based *model independent quadratic programming* (MIQP) control as the feedback term while using the impedance control as the feed-forward input.

A. Impedance Control for Prosthesis

Impedance Control. Based on the notion of impedance control first proposed by Hogan [13], the torque at each joint during a single step can be piecewisely represented by a series of passive impedance functions [19] with the form:

$$\tau = k(\theta - q^e) + b\dot{\theta}, \quad (6)$$

where, k , q^e and b represent the stiffness, equilibrium angle and damping respectively, which are constant for specific phase. This formula only requires local information about the controlled prosthetic joint—in this case the right knee joint ($\theta_{RK}, \dot{\theta}_{RK}$)—so the end result is a simple prosthesis control. In particular, since the direct control input is voltage in AMBER, we can represent the joint input voltage during a single step by this function piecewisely with the form:

$$V_p^{imp} = k(\theta - q^e) + b\dot{\theta}, \quad (7)$$

where V_p^{imp} is termed the impedance voltage.

Phase Separation. While impedance control with a finite state machine is one of the most widely used algorithms suggested to date [15], one main problem is to identify the phases correctly during a single step.

Based on the previous work [3], even though a point feet model is considered, analysis of AMBER walking data shows that one gait cycle can be divided into four phases based on the prosthesis knee joint, which are denoted as $p = \{1, 2, 3, 4\}$, as shown in Fig. 2. Specifically, each phase begins at time t_0^p and ends at t_f^p . The phase separation principle is similar to that in [3] but with values specific

to the gait of AMBER. Therefore, in each phase p , the dynamics of the biped system can be stated as:

$$\begin{cases} D(\theta)\ddot{\theta} + H_v(\theta, \dot{\theta}) = B_v V_{in} & \forall t \in [t_0^p, t_f^p], \\ (\theta(t_0^p), \dot{\theta}(t_0^p)) = R(\theta(t_f^{p-1}), \dot{\theta}(t_f^{p-1})). \end{cases} \quad (8)$$

where $p-1$ is set to 4 if $p=1$ and the switching function R has been defined as follows:

$$R(\theta(t), \dot{\theta}(t)) = \begin{cases} \Delta(\theta(t), \dot{\theta}(t)) & \text{at impacts,} \\ (\theta(t), \dot{\theta}(t)) & \text{otherwise.} \end{cases} \quad (9)$$

Specifically, for the prosthesis joint, we will replace the corresponding V_{in} term (denoted as $V_{in,p}$) with the prosthetic voltage input V_p^{imp} , which can be represented as:

$$V_{in,p} := V_p^{imp} = k_p(\theta_{RK}(t) - q_p^e) + b_p \dot{\theta}_{RK}(t), \quad (10)$$

where $\theta_{RK}(t)$ and $\dot{\theta}_{RK}(t)$ denote angle and angular velocity of the right knee at time t . The end result is the following construction for the prosthetic joint:

$$D^j(\theta)\ddot{\theta} + H_v^j(\theta, \dot{\theta}) = V_{in,p} \quad \forall t \in [t_0^p, t_f^p], \quad (11)$$

where i indicates the i^{th} row of the corresponding term, which will be updated according to the phase p . Note that, since we define the body coordinates based on the stance and non-stance nomenclature, we have $i=5$ when $p=1, 2$, i.e., the prosthetic device is the non-stance leg, and $i=2$ while $p=3, 4$, i.e., the prosthetic device is the swing leg.

Impedance Parameter Estimation. With the phase transitions defined above, another problem of impedance control is to identify the control parameters for each phase. In the previous work [3], the authors showed that the impedance parameters for a lower-limb prosthesis can be learned by the observation of unimpaired human walkers. The results have been validated both in simulation and in experiment with a transfemoral prosthetic device. In this work, instead of using the experimental data from the robot, we extend the method to estimate the impedance parameters by observing the simulated “unimpaired” walking data of AMBER.

Through the use of human-inspired optimization and the essential model recovery algorithm to characterize the actual physical model, the estimation algorithm does not require experimental data, as a result, can potentially save the difficulty of experimental tuning of the devices. The estimated impedance parameters are shown in Table I, and the estimation algorithm is omitted here due to space constraints.

B. CLF Model Independent QP

In this part, a brief revisit of human-inspired control will be given first (additional details can be found in [23]). Based on this foundational work and inspired by the CLF controller in [6], we will discuss the novel CLF based model independent control in detail.

Human-Inspired Control Revisit. Motivated by the goal of achieving human-like bipedal robotic walking, human-inspired control aims to drive the actual robot outputs $y_a(\theta)$, which are functions of joint angles, to the desired human outputs $y_d(t, \alpha)$ that can be represented by the *canonical walking*

function (CWF) introduced in [4]. Therefore, motivating the introduction of human-inspired outputs:

$$y(\theta, \dot{\theta}) = \begin{bmatrix} y_1(\theta, \dot{\theta}) \\ y_2(\theta) \end{bmatrix} = \begin{bmatrix} y_1^a(\theta, \dot{\theta}) - v_{hip} \\ y_2^a(\theta) - y_2^d(\tau(\theta), \alpha) \end{bmatrix}, \quad (12)$$

where α is the set of parameters of CWF and $\tau(\theta)$ is the parameterized time. $y_1(\theta, \dot{\theta})$ is the relative degree one output, which is the difference between the actual forward hip velocity $y_1^a(\theta, \dot{\theta})$ and the desired hip velocity v_{hip} . $y_2(\theta)$ are the relative degree two human-inspired outputs which are the differences between the actual outputs $y_2^a(\theta)$ and the desired outputs $y_2^d(\tau(\theta), \alpha)$.

With this in hand, the dynamics in (4) can be obtained as:

$$\begin{bmatrix} \dot{y}_1 \\ \dot{y}_2 \end{bmatrix} = \underbrace{\begin{bmatrix} L_f y_1(\theta, \dot{\theta}) \\ L_f^2 y_2(\theta, \dot{\theta}) \end{bmatrix}}_{L_f} + \underbrace{\begin{bmatrix} L_g y_1(\theta, \dot{\theta}) \\ L_g L_f y_2(\theta, \dot{\theta}) \end{bmatrix}}_A u, \quad (13)$$

where L_f is the Lie derivative and A is dynamic decoupling matrix, which is nonlinear in most cases. By picking:

$$u = A^{-1}(L_f + \mu), \quad (14)$$

the equation (13) turns into the linear form:

$$\begin{bmatrix} \dot{y}_1 \\ \dot{y}_2 \end{bmatrix} = \mu. \quad (15)$$

By designing μ properly, [4] for example, one can drive both $y_1 \rightarrow 0$ and $y_2 \rightarrow 0$ exponentially; as a result, human-inspired walking can be achieved.

This control strategy works for nonlinear systems, but requires good knowledge about the model. In the domain of complex nonlinear robotic control, this assumption is usually not satisfied, and therefore yields the computed torque to be far away from the required torque. PID control still dominates in real world control problems since it does not require accurate model information, i.e., it is model independent. However, considering all the well-known problems of PID control (hand tuning, none optimal [7]), we are motivated to find a new optimal control strategy to overcome these issues while maintaining the model insensitiveness property. To achieve this goal, the approach of this work will be introduced as follows.

CLF MIQP. By defining the vector $\eta = (y, \dot{y})^T \in \mathbb{R}^{2 \times 1}$, equation (15) can be reformulated as:

$$\dot{\eta} = \underbrace{\begin{bmatrix} 0 & 1 \\ 0 & 0 \end{bmatrix}}_F \eta + \underbrace{\begin{bmatrix} 0 \\ 1 \end{bmatrix}}_G \mu. \quad (16)$$

In the context of this control system, we consider the continuous time algebraic Riccati equation with $P = P^T > 0$:

$$F^T P + P F - P G G^T P + I = 0, \quad (17)$$

that yields the optimal solution $\mu = -G^T P \eta$.

With the aim to have stronger bounds of the convergence of the considered hybrid system, we take this method further by defining $\eta_\varepsilon = (y/\varepsilon, \dot{y})^T$. We then choose P and $\varepsilon > 0$ carefully to construct a *rapidly exponentially stabilizing*

control Lyapunov function (RES-CLF) that can be used to stabilize the system in a rapidly exponentially fashion [6]. Particularly, we define the positive definite CLF as:

$$V_\varepsilon(\eta) = \eta^T \begin{bmatrix} \frac{1}{\varepsilon} I & 0 \\ 0 & I \end{bmatrix} P \begin{bmatrix} \frac{1}{\varepsilon} I & 0 \\ 0 & I \end{bmatrix} \eta := \eta^T P_\varepsilon \eta. \quad (18)$$

Differentiating this function renders:

$$\dot{V}_\varepsilon(\eta) = L_f V_\varepsilon(\eta) + L_g V_\varepsilon(\eta) \mu, \quad (19)$$

where $L_f V_\varepsilon(\eta) = \eta^T (F^T P_\varepsilon + P_\varepsilon F) \eta$, $L_g V_\varepsilon(\eta) = 2\eta^T P_\varepsilon G$.

In order to exponentially stabilize the system, we want to find μ such that, for specifically picked $\gamma > 0$ [6], we have:

$$L_f V_\varepsilon(\eta) + L_g V_\varepsilon(\eta) \mu \leq -\frac{\gamma}{\varepsilon} V_\varepsilon(\eta). \quad (20)$$

Therefore, an optimal μ could be found by solving the following minimization problem:

$$m(\eta) = \operatorname{argmin}\{\|\mu\| : \varphi_0(\eta) + \varphi_1(\eta)\mu \leq 0\}, \quad (21)$$

which is equivalent to solving the quadratic program (QP):

$$m(\eta) = \operatorname{argmin}_{\mu \in \mathbb{R}^{n_1+n_2}} \mu^T \mu \quad (22)$$

$$\text{s.t. } \varphi_0(\eta) + \varphi_1(\eta)\mu \leq 0, \quad (\text{CLF})$$

where $\varphi_0(\eta) = L_f V_\varepsilon(\eta) + \frac{\gamma}{\varepsilon} V_\varepsilon(\eta)$ and $\varphi_1(\eta) = L_g V_\varepsilon(\eta)$. n_1 , n_2 correspond to the number of relative degree one outputs and relative degree two outputs. In this case, we have $n_1 = 0$ and $n_2 = 1$ since we are only considering the knee joint.

Note that, instead of substituting the optimal solution μ into equation (14) to obtain the feedback control law as in [6], we use μ directly as control input into the original system without considering the model decoupling matrix A and L_f . Therefore, we term this control strategy *model independent quadratic program* (MIQP) controller.

Taking a further look into the MIQP algorithm, we basically constructed a new linear control system (16) that only focuses on the errors between the actual outputs and desired outputs, while not requiring any information about the original model. Another immediate advantage is that the torque bounds can be directly applied in this formulation where, the optimal control value can be obtained while respecting the torque bounds. As discussed in [5], this can be achieved by relaxing the CLF constraints with a large penalty value $\rho > 0$. In particular, we consider the MIQP as:

$$\operatorname{argmin}_{(\delta, \mu) \in \mathbb{R}^{n_1+n_2+1}} \rho \delta^2 + \mu^T \mu \quad (23)$$

$$\text{s.t. } \varphi_0(\eta) + \varphi_1(\eta)\mu \leq \delta, \quad (\text{CLF})$$

$$\mu \leq \mu_{MAX}, \quad (\text{Max Torque})$$

$$-\mu \leq \mu_{MAX}. \quad (\text{Min Torque})$$

Similarly, μ can be replaced with the voltage V^{qp} directly without affecting the configuration of this algorithm.

MIQP+Impedance Control. Utilizing the formal framework discussed above, we are now ready to introduce another main result of this paper, which is the MIQP+Impedance controller for prosthesis control.

While MIQP control benefits from its model independence property in an optimal fashion, it also suffers from the overshoot problem as the PID controller does because of the lack of model information. Particularly, this issue can be a fatal problem for a prosthesis controller with the safety consideration of the amputee; therefore, this motivates the introduction of MIQP+Impedance control. With the impedance control V_p^{imp} as the feed-forward term, the input voltage of the prosthetic leg $V_{in,p}$ in (11) can be stated as: $V_{in,p} = V^{qp} + V_p^{imp}$ with V^{qp} the voltage computed from the MIQP problem. To take a further step, we add the impedance term V_p^{imp} into the MIQP construction, which yields the following MIQP+Impedance problem:

$$\begin{aligned} & \underset{(\delta, V^{qp}) \in \mathbb{R}^2}{\operatorname{argmin}} \quad \rho \delta^2 + V^{qpT} V^{qp} & (24) \\ & \text{s.t.} \quad \varphi_0(\eta) + \varphi_1(\eta) V^{qp} \leq \delta + \varphi_1(\eta) V_p^{imp}, & (\text{CLF}) \\ & \quad V^{qp} \leq V_{MAX}^{qp}, & (\text{Max QP Voltage}) \\ & \quad -V^{qp} \leq -V_{MAX}^{qp}, & (\text{Min QP Voltage}) \\ & \quad V^{qp} \leq V_{MAX} - V_p^{imp}, & (\text{Max Input Voltage}) \\ & \quad -V^{qp} \leq V_{MAX} + V_p^{imp}. & (\text{Min Input Voltage}) \end{aligned}$$

By adding the impedance feed-forward term into the QP problem, the model independent control gathers model information, therefore can adjust the V^{qp} accordingly to accommodate the feed-forward term in order to achieve exceptional tracking. By setting the QP voltage bounds V_{MAX}^{qp} , we can limit the overshoot problem. Note that, we also set the total input voltage bounds for the QP problem such that the final total optimal input voltage $V_{in,p}$ will satisfy the input voltage bounds which are constrained by the hardware.

IV. PROSTHETIC WALKING IN SIMULATION

With the control architecture in hand, the simulation results of AMBER will be discussed in this section. The tracking results of the prosthesis joint by using different controllers will be compared. Finally, robustness tests will also be performed and compared with using different controllers.

A. Tracking Performance with Different Controllers

With the exception of the prosthesis joint, on which different controllers will be implemented, the remaining joints will be controlled with the human-inspired voltage P control.

Three different controllers are tested as the prosthetic controller: P control, impedance control and MIQP+Impedance control. Fig. 6 shows the tracking performances of the prosthesis knee joint using these three controllers. Using the tracking results of P control as the nominal reference as shown in Fig. 6a, we can see that the MIQP+Impedance control improves the tracking performance for both stance and non-stance phases by more than 10 times w.r.t the *RMS* error, while impedance control yields worse tracking results.

The phase portrait for 32 steps with utilizing voltage P control can be seen in Fig. 3, which clearly shows the convergence to one periodic orbit since the controls are same on both of the legs. The phase portrait for 64 steps with using MIQP+Impedance can be seen in Fig. 4, showing

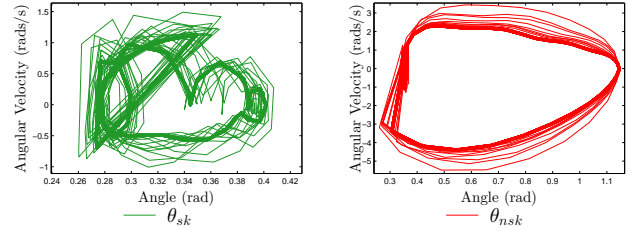


Fig. 3: Phase portrait of prosthesis joint with voltage control

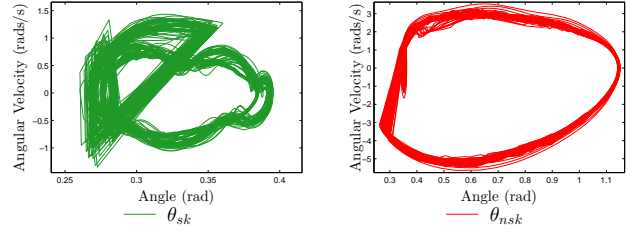


Fig. 4: Phase portrait of prosthesis joint with MIQP+Impedance control

that the phase portrait converges to two limit cycles since the controllers are asymmetric. The simulation gait tiles of two steps walking with using both impedance control and MIQP+Impedance control are shown in Fig. 7 and Fig. 8, respectively. Note that, the robot can only walk 12 steps with only impedance control in simulation. This is reasonable since we consider underactuated ankles in this work. Impedance control is fundamentally passive and not able to correct tracking errors efficiently, therefore, any small error in tracking may lead to a failure to walk.

With the comparisons above, we can conclude that MIQP+Impedance controller delivers improved tracking performance without increasing the torque requirement, which is the key perspective while evaluating a prosthetic controller.

B. Stability Testing

Stability is another fundamental requirement for a prosthetic controller. With the proposed MIQP+Impedance control, we claim that this controller renders more robustness than just impedance control, and therefore is safer for the amputee's daily use. Two robustness tests are applied to the robot in simulation; one is to add an instantaneous push and another one is to let the robot walk above an obstacle.

Reaction to impulse push. A $2N$ impulse force (lasting for 0.05s) has been applied to the prosthetic leg while

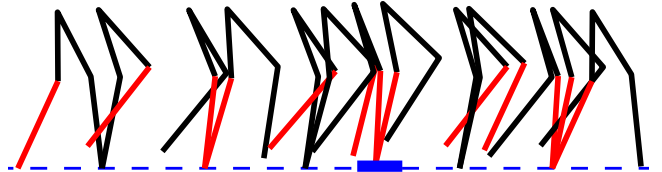


Fig. 5: Gait tiles of walking over an obstacle with MIQP+Impedance control.

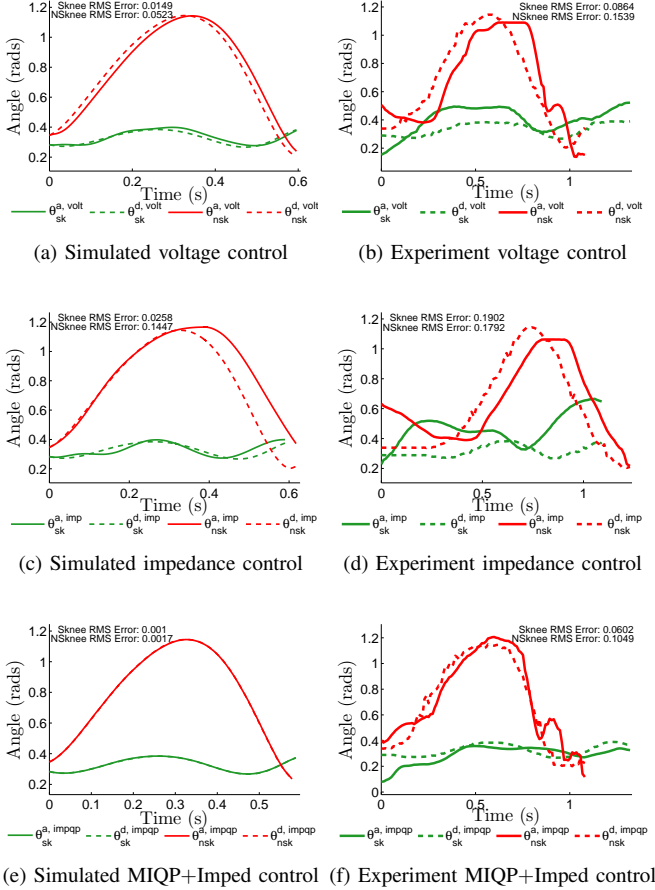


Fig. 6: Actual and desired outputs of the prosthesis knee joint with different controllers in both simulation (left) and experiment (right).

it's in the swing phase. From the video [1], we can see that the prosthetic device with the proposed controller can tolerate this disturbance and maintain good tracking. We also tested the same disturbance when using only the impedance controller; the tracking error becomes bigger due to the disturbance and the robot falls after 6 steps.

To overcome an obstacle. In the simulation, we let the robot walk over a 20 mm height obstacle. The gait tiles can be seen in Fig. 5, showing that the robot can overcome the obstacle smoothly. A similar test is also conducted with only impedance control. The robot can walk over the obstacle, however, the tracking performance becomes worse. Both the tests are shown in the video [1] with details.

TABLE I: Impedance Parameters of the Prosthesis.

Sim/Exp	Estimated parameters			Experimental parameters		
Phase	$k_p[V]$	$b_p[V\cdot s]$	$q_p^0[\text{rad}]$	$k_p[V]$	$b_p[V\cdot s]$	$q_p^0[\text{rad}]$
P1	-3.9731	0.1242	0.2493	-12.9731	0.0242	0.1283
P2	-3.7714	0.1499	0.2327	-18.7714	0.0499	0.1
P3	-0.2123	0.1405	1.1378	-15.212	0.1405	1.1405
P4	-0.1956	0.1418	0.1999	-18.5568	0.0044	0.1024

V. EXPERIMENTAL IMPLEMENTATION AND RESULTS

In this section, the controllers are tested on the physical robot AMBER. The experiments show similar results as in simulation—that is, the MIQP+Impedance controller yields better tracking performance and more robustness.

A. Impedance Control

Starting with the estimated impedance parameters obtained from simulation, we are able to tune the parameters within a small range and get sustainable walking by only using the impedance controller. The actual impedance parameters used on the robot are shown in Table I. Note that, the actual impedance parameters k_p are bigger than the estimated values and the impedance parameters b_p are tuned to be low. The main reasons are twofold. Firstly, in simulation, the friction and damping of the transmission, i.e., the motor and gear box, are not considered. Therefore, higher k_p parameters are required to compensate for the model differences. The second reason is that the angular velocity information from AMBER is not accurate, bordering being unusable, which prevents the use of the velocity terms. Therefore, b_p terms has to be lowered, which, as a result, leads to higher k_p parameters in order to provide enough torque.

Besides the discussion above, we claim that the estimated impedance parameters can capture the essentials of the physical model, thus the requirement of hand tuning can be kept to minimum. The tracking result of using impedance controller can be seen in Fig. 6d. Compared to the tracking of P control as shown in Fig. 6b, the impedance control shows worse tracking performance.

B. MIQP+Impedance Control

Using the tuned impedance parameters from previous section, we apply the impedance control as the feed-forward term while using the MIQP as the feedback term to correct the tracking errors and reject the disturbances. From Fig. 6f, we can see the tracking with using MIQP+Impedance controller is the best among the three methods in both stance phase and non-stance phase (RMS error reduced by more than 50% for both phases). We also tested the robustness of the walking with MIQP+Impedance control, the robot was able to overcome a 40 mm height block and could stand for big pushes on the prosthetic leg. The details can be seen in the video [1]. Note that, in the video, the walking gait using MIQP+Impedance control is not as smooth as that with using only voltage P control. This is because of the asymmetric control and the fact that the prosthetic joint has better tracking than the healthy joint.

VI. CONCLUSIONS

In this work, we first proposed a new method which is to test and design the prosthetic controllers on a robot that has been shown to have qualitatively human-like walking [4]. Since the physical robot displays human-like walking gait, which captures the essentials of human locomotion, we claim that testing the prosthetic controller (or device) in such

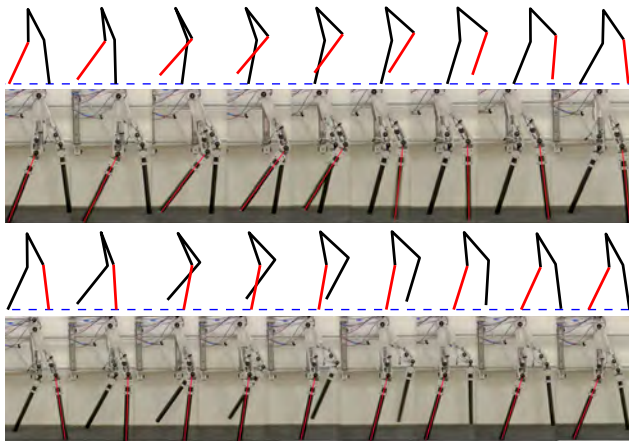


Fig. 7: Experimental and simulation gait tiles with only impedance controller. Red line indicates the prosthesis.

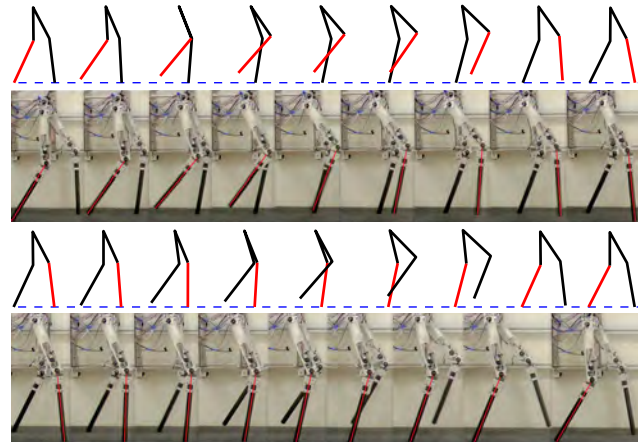


Fig. 8: Experimental and simulation gait tiles using MIQP + Impedance control. Red line indicates the prosthesis.

a robot will yield qualitative information, and therefore, can help improve the designs of both the prosthetic controller and the lower-limb prosthetic device. Then, a novel optimal prosthesis control algorithm: MIQP+Impedance control was introduced to control the prosthetic device with the framework discussed above. This controller benefits from both the feed-forward impedance control that gives model information and the MIQP method that renders model independent control in an optimal fashion that is inherited from the CLF based QP control method. This controller has been verified on the robot in both simulation and experiment. Compared with the other two control methods, the proposed optimal controller shows the best tracking performance with the same level of energy input. The robustness tests also show that this optimal controller can overcome disturbances and obstacles while maintaining good tracking.

The limitations of this work are mainly due to the hardware of the robot. AMBER doesn't have feet and the ankles are underactuated. Also, the velocity sensor data is not usable, which limits the performance of the MIQP algorithm. In future work, we are going to test the same algorithm on the footed robot AMBER2 which has achieved good human-like walking with both knee and ankle actuation [2].

REFERENCES

- [1] Experimental and simulation results. <http://youtu.be/5TuTyKhMniU>.
- [2] Sustainable multi-domain walking of amber2. <http://youtu.be/VvkIdCK1L54>.
- [3] Navid Aghasadeghi, Huihua Zhao, Levi J Hargrove, Aaron D Ames, Eric J Perreault, and Timothy Bretl. Learning impedance controller parameters for lower-limb prostheses. *IEEE: IROS*, 2013.
- [4] A. D. Ames. First steps toward automatically generating bipedal robotic walking from human data. In *8th International Workshop on Robotic Motion and Control, RoMoCo'11*, Bukowy Dworek, 2011.
- [5] A. D. Ames and M. J. Powell. Towards the unification of locomotion and manipulation through control lyapunov functions and quadratic programs. In *Springer's Lecture Notes in Control and Information Science series*, 2013.
- [6] A.D. Ames, K. Galloway, and J.W. Grizzle. Control lyapunov functions and hybrid zero dynamics. In *Decision and Control (CDC), 2012 IEEE 51st Annual Conference on*, pages 6837–6842.
- [7] D.P. Atherton and S. Majhi. Limitations of pid controllers. In *American Control Conference*, pages 3843–47, 1999.
- [8] Christopher G Atkeson and Stefan Schaal. Robot learning from demonstration. In *ICML*, volume 97, pages 12–20, 1997.
- [9] Samuel Au, Max Berniker, and Hugh Herr. Powered ankle-foot prosthesis to assist level-ground and stair-descent gaits. *Neural Networks*, 21(4):654 – 666, 2008.
- [10] S.K. Au, P. Bonato, and H. Herr. An emg-position controlled system for an active ankle-foot prosthesis: an initial experimental study. In *IEEE on 9th ICORR, 2005*, pages 375–9.
- [11] J.A. Blaya and H. Herr. Adaptive control of a variable-impedance ankle-foot orthosis to assist drop-foot gait. *Neural Systems and Rehabilitation Engineering, IEEE Transactions on*, 12(1):24–31, 2004.
- [12] Joseph Hitt, A Mehmet Oymagil, Thomas Sugar, Kevin Hollander, Alex Boehler, and Jennifer Fleeger. Dynamically controlled ankle-foot orthosis (dco) with regenerative kinetics: incrementally attaining user portability. In *IEEE International Conference on Robotics and Automation*, pages 1541–46. IEEE, 2007.
- [13] Neville Hogan. Impedance control: An approach to manipulation. pages 304–313, 1984.
- [14] Y. Hürmüzlü and D. B. Marghitu. Rigid body collisions of planar kinematic chains with multiple contact points. *Intl. J. of Robotics Research*, 13(1):82–92, February 1994.
- [15] René Jimenez-Fabian and Olivier Verlinden. Review of control algorithms for robotic ankle systems in lower-limb orthoses, prostheses, and exoskeletons. *Medical engineering & physics*, 34(4):397–408.
- [16] Jun Nakanishi, Jun Morimoto, Gen Endo, Gordon Cheng, Stefan Schaal, and Mitsuo Kawato. Learning from demonstration and adaptation of biped locomotion. *Robotics and Autonomous Systems*, 47(2):79–91, 2004.
- [17] Aykut Mehmet Oymagil, Joseph K Hitt, Thomas Sugar, and Jennifer Fleeger. Control of a regenerative braking powered ankle foot orthosis. In *IEEE on 10th ICORR, 2007*, pages 28–34. IEEE.
- [18] Dejan Popovic, Rajko Tomovic, Dejan Tepavac, and Laszlo Schwirtlich. Control aspects of active above-knee prosthesis. *International Journal of Man-Machine Studies*, 35(6):751 – 767, 1991.
- [19] Frank Sup, Amit Bohara, and Michael Goldfarb. Design and Control of a Powered Transfemoral Prosthesis. *The International journal of robotics research*, 27(2):263–273, February 2008.
- [20] Frank Sup, Huseyin Atakan Varol, and Michael Goldfarb. Upslope walking with a powered knee and ankle prosthesis: initial results with an amputee subject. *IEEE transactions on neural systems and rehabilitation engineering*, 19(1):71–8, February 2011.
- [21] Radcliffe C. W. Biomechanical basis for the design of prosthetic knee mechanisms. *Rehabilitation Engineering International Seminar*, 1980.
- [22] Shishir Nadubettu Yadukumar, Murali Pasupuleti, and Aaron D Ames. From formal methods to algorithmic implementation of human inspired control on bipedal robots. In *Algorithmic Foundations of Robotics X*, pages 511–526. Springer, 2013.
- [23] H. Zhao, M. J. Powell, and A. D Ames. Human-inspired motion primitives and transitions for bipedal robotic locomotion in diverse terrain. In *Optim. Control Appl. Meth.*, 2013.